

1 Nuclear modification factor of inclusive charged particles
2 in Au+Au collisions at $\sqrt{s_{NN}} = 27$ GeV with the STAR
3 experiment

4 Aitbayev Alisher (*for the STAR Collaboration*)

5 Joint Institute for Nuclear Research (JINR)

6 December 27, 2023

7 **Abstract**

8 The Beam Energy Scan (BES) program at RHIC aims to explore the QCD phase
9 diagram, including the search for the evidence of the 1st order phase transition from
10 hadronic matter to Quark-Gluon Plasma (QGP) and the location of the QCD critical point.
11 One of the features previously observed in the study of QGP is the effect of suppression of
12 particle production with high transverse momenta p_T (> 2 GeV/c) at energies $\sqrt{s_{NN}} =$
13 62.4 - 200 GeV [1], which was deduced from the charged-particle nuclear modification factor
14 (R_{CP}) measured using the data from Beam Energy Scan Program Phase I (BES-I) of STAR
15 experiment. In 2018, STAR has collected over 500 million events from $Au+Au$ collisions
16 at $\sqrt{s_{NN}} = 27$ GeV as a part of the STAR BES-II program, which is about a factor of
17 10 higher than BES-I 27 GeV data size. In this report, we present new measurements of
18 charged particle production and the nuclear modification factor R_{CP} , from this new 27
19 GeV data set and compare them with the BES-I results. The new measurements extend
20 the previous BES-I results to higher transverse momentum range, which allows better
21 exploration of the jet quenching effects at low RHIC energies, and may help to understand
22 the effects of the formation and properties of QGP at these energies.

Introduction

Collisions of heavy ions at high energies create a dense, strongly interacting, deconfined partonic fluid called quark-gluon plasma (QGP) [2, 3, 4, 5]. Quantifying the properties of QGP is necessary for the description of the Quantum ChromoDynamics (QCD) phase diagram [6], as well as constraining parameters in cosmological models that describe the evolution of the universe through the QCD phase diagram [7]. The most common way to characterize the QCD phase diagram in heavy-ion experiments [8] is in the temperature (T) and baryon chemical potential plane [9]. High collision energies correspond to low initial baryon chemical potentials (μ_B), while low collision energies lead to high values of μ_B [10]. The crossover behavior at low μ_B region is predicted by the Lattice QCD (LQCD) calculations [11, 12], while a first-order phase transition is predicted at sufficiently large μ_B [13, 14], which would imply the existence of the critical end-point.

To experimentally study the phase structure of QCD matter as a function of T and μ_B , the Relativistic Heavy Ion Collider (RHIC) has launched the Beam Energy Scan (BES) program. The essence of the program is to carry out collisions at different energies, thereby creating systems with different initial conditions of T and μ_B to search for the critical point of the phase diagram. The graph in Fig. (1) shows the QCD phase diagram with mapping of the available experimental areas reached at different collision energies during all phases of the BES program. By creating diverse initial states, we aim to achieve the intersection of different reaction trajectories with the phase boundary at various values of T and μ_B . This will allow us to explore interesting features of the phase diagram, including the conjectured critical point and the first-order phase transition.

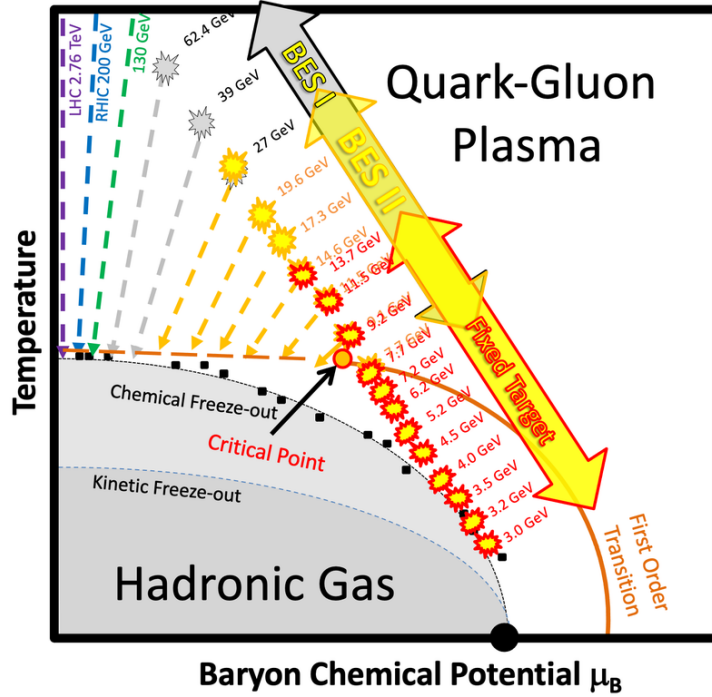


Figure 1: QCD phase diagram in terms of the temperature T and baryon chemical potential μ_B with BES-I, BES-II, and FXT access areas marked together with the hypothesized location of the phase boundary and Critical Point [15].

45 The suppression effect of charged particle production with high transverse momenta ($p_T >$
46 $2 \text{ GeV}/c$) is one of the most interesting results observed at the Solenoidal Tracker At RHIC
47 (STAR) experiment during the BES-I program. This effect has been interpreted as the increase
48 in energy loss of partons in the quark-gluon plasma produced at high energy heavy ion-collisions.
49 It is commonly referred to as jet quenching in dense partonic matter [16, 17] and was predicted
50 as a sign of the formation of the QGP phase, where simple model of hadron scattering cannot
51 describe the observations. This effect can be quantified using the nuclear modification factor
52 R_{CP} . The nuclear modification factor (R_{CP}) can be experimentally calculated as follows:

$$R_{CP} = \frac{\langle N_{coll} \rangle_{Peripheral} \left(\frac{d^2 N}{dp_T d\eta} \right)_{Central}}{\langle N_{coll} \rangle_{Central} \left(\frac{d^2 N}{dp_T d\eta} \right)_{Peripheral}} \quad (1)$$

53 In this context, $\langle N_{coll} \rangle$ denotes the mean number of binary collisions within a specific cen-
54 trality class, and it can be approximated through the use of a Glauber Monte Carlo simulation
55 [18]. If we consider heavy-ion collisions as a combination of N_{coll} independent binary nucleon-
56 nucleon collisions, the R_{CP} value would be equal to 1 across the entire transverse momentum
57 (p_T) range. Effects that elevate the particle yield per binary collision in central heavy-ion
58 collisions compared to $p+p$ or peripheral collisions are collectively referred to as enhancement
59 effects, resulting in $R_{CP} > 1$. Conversely, those that diminish the particle yield are known

60 as suppression effects, leading to $R_{CP} < 1$. Consequently, R_{CP} provides insight into whether
61 enhancement or suppression effects dominate, although it does not quantify their magnitudes
62 separately. Equation (1) compares the particle production at very small impact parameters
63 (central class), where the mean path length through the produced nuclear medium might be
64 longer, with that at very large impact parameters (peripheral class), where shorter in-medium
65 path lengths should yield smaller energy loss [1].

66 Certain physical effects can boost hadron production in specific kinematic ranges, effectively
67 masking suppression due to the jet quenching. One such effect is the Cronin effect, a Cold
68 Nuclear Matter (CNM) phenomenon first observed in asymmetric collisions involving heavy and
69 light nuclei, where an amplification of high p_T particles was measured instead of suppression
70 [19, 20, 21]. Studies indicate that the Cronin effect's enhancement increases as the impact
71 parameter decreases [22, 23]. Other processes in heavy-ion collisions, such as radial flow and
72 particle coalescence, can also induce enhancement [24]. This is associated with the effect of
73 increasing particle momenta in steeply falling spectra. The transition of more abundant low
74 p_T particles towards higher momenta in more central events, as seen in radial flow, p_T -ridge
75 formation, or coalescence, leads to an enhancement of the nuclear modification factor (R_{CP}).
76 It is expected that these enhancement effects will compete with jet quenching, which shifts
77 high- p_T particles towards lower momenta. Therefore, observing a nuclear modification factor
78 exceeding unity does not automatically imply the absence of quark-gluon plasma formation.
79 Resolving these competing effects can be accomplished using additional methods, such as event-
80 plane-dependent nuclear modification factors [1]. Figure (2) illustrates the nuclear modification
81 factor measured for inclusive charged hadrons produced in $Au+Au$ collisions during the BES-I
82 program [1]. At high transverse momenta ($p_T > 2GeV/c$), there is a gradual transition from
83 strong enhancement to strong suppression with increasing collision energies.

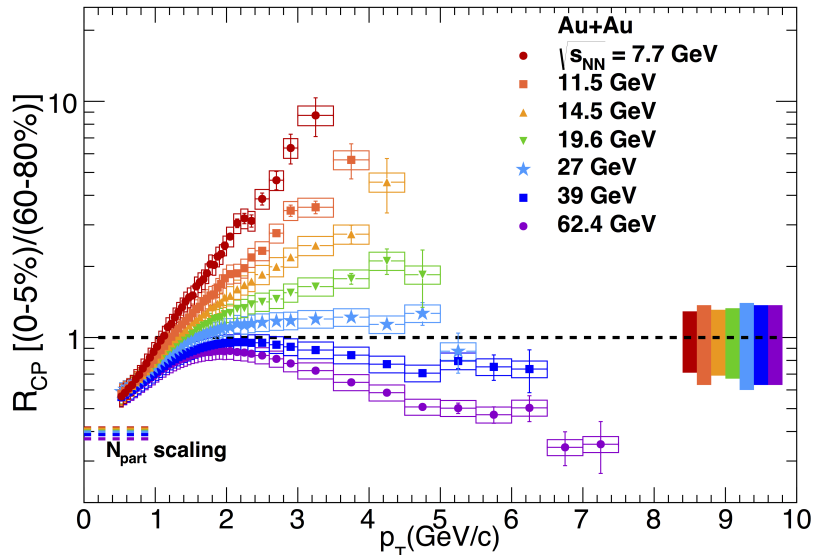


Figure 2: Unidentified charged hadron R_{CP} for RHIC BES-I and high energy data. The uncertainty bands at unity on the right side of the plot correspond to the p_T independent uncertainty in N_{coll} scaling with the color in the band corresponding to the color of the data points for that energy. The vertical uncertainty bars correspond to statistical uncertainties and the boxes to systematic uncertainties. [1]

84 In this report, preliminary results of the nuclear modification factor for $Au+Au$ collisions
 85 at collision energy of $\sqrt{s_{NN}} = 27$ GeV from the STAR BES-II program will be presented.

86 Data Analysis

87 The data under analysis was collected in 2018 from $Au+Au$ collisions at a center-of-mass
 88 energy of $\sqrt{s_{NN}} = 27$ GeV during the BES-II at RHIC runs by the STAR detector. The TPC
 89 and TOF subsystems of STAR provide tracking and particle identification for our analysis.
 90 To measure momentum, these detectors operate in a magnetic field with an intensity of 0.5
 91 T, allowing the trajectory of passing charged particles to be bent. In combination with the
 92 path length of trajectories measured in the TPC and the time of flight from the TOF, this
 93 provides information on the speed of charged particles, denoted as $1/\beta$, which is used for
 94 particle identification. $1/\beta$ is determined as $\sqrt{(\frac{mc}{p})^2 + 1}$, where m is the particle mass, p is the
 95 particle momentum, and c is the time of flight. Centrality is determined by the charge particle
 96 multiplicity at mid-rapidity in the TPC. Events at low energies caused by ion interactions
 97 with the beam pipe were excluded by introducing a restriction along the XY plane ($V_r =$
 98 $\sqrt{V_x^2 + V_y^2} < 2cm$). Additionally, only events within a range of 75 cm (-75;75 cm) along the Z
 99 axis were selected to consider only particles formed at the central region of the detector. To
 100 reduce the contribution of particles from secondary interactions and weak decays, only tracks
 101 with a distance of closest approach (DCA) from the primary vertex of less than 2 cm were

102 chosen. We require tracks to fall in the pseudorapidity range $|\eta| < 1$ to ensure that all selected
 103 tracks pass entirely through the central part of the TPC. The parameter `nHitsFit` represents
 104 the number of hits that can be used to reconstruct a track. Increasing the number of hits in
 105 a track improves momentum resolution, but requiring a very large number of hits reduces the
 106 quality of tracks with low transverse momentum p_T values. It has been determined that a
 107 minimum of 16 hits is a good value for this analysis, and the ratio of the number of points used
 108 in track reconstruction to the number of possible points (`nFitOverPoss`) should be greater than
 109 0.52 to prevent split tracks. The p_T and species-dependent tracking efficiencies in the TPC
 110 were determined by propagating Monte Carlo particle tracks through a simulation of STAR
 111 detector and embedding the generated signals into real events for each energy and centrality.
 112 The charged hadron tracking efficiency was then taken as the weighted average of fits to the
 113 single species efficiencies with weights provided by fits to the corrected spectra of each species.
 114 This method allowed for extrapolation of charged hadron efficiencies to higher p_T than the
 115 single species spectra could identify. The efficiencies are constant as a function of p_T in the
 116 extrapolated region, limiting the impact from the extrapolation on the systematic uncertainties.
 117 The systematic errors were calculated by varying the selection criteria. The analysis cuts
 118 used to estimate systematic uncertainties are listed below:

Systematic sources	Default	Variation(s)
Vertex_R	2	1-3 [cm]
Vertex_Z	75	65-70 [cm]
DCA	2	1.5-2.5 [cm]
nHitsFit	16	12-20
nFitOverPoss	0.5	0.6

119 Results and Discussion

120 The transverse momentum particle spectra for $Au+Au$ collisions at energy of $\sqrt{s_{NN}} = 27$ GeV
 121 for inclusive charged particles in different centrality classes are shown in Fig. (3).

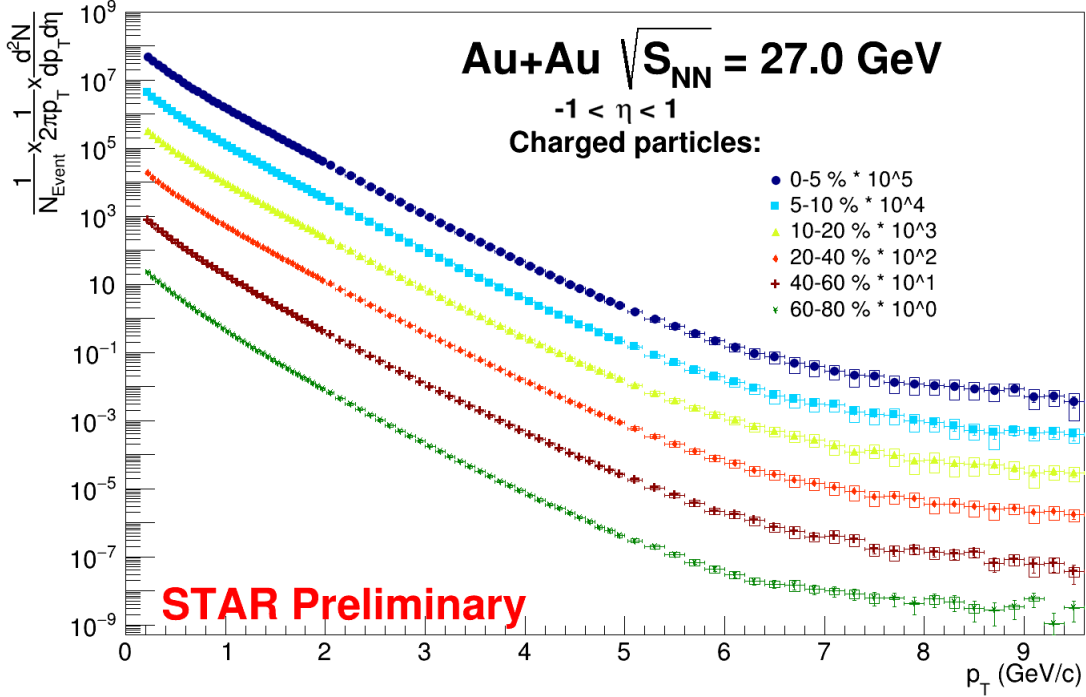


Figure 3: Transverse momentum distribution of inclusive charged particles for collision energy of 27 GeV. Each spectrum corresponds to a certain centrality class and is multiplied by coefficient from $1 - 10^5$ for visibility. The vertical error bars correspond to statistical uncertainties and the colored boxes to the systematic uncertainties.

122 The spectrum are shown for six centrality classes, where the upper spectra corresponds to
 123 the 0-5% centrality and decrease for more peripheral collisions. Each set of data points was
 124 multiplied by a constant for visibility.

125 From Fig. (3), it can be noticed that in the BES-II program, the spectra have a greater
 126 coverage in terms of transverse momentum p_T for all centrality classes, which enables a more
 127 comprehensive investigation of the nuclear modification factor.

128 Figure (4) demonstrates the R_{CP} for $Au+Au$ collisions at a collision energy of 27 GeV, for
 129 the pseudorapidity range of $-1 < \eta < 1$. The R_{CP} was calculated as:

$$R_{CP} = \frac{\langle N_{coll} \rangle_{Peripheral}}{\langle N_{coll} \rangle_{Central}} \frac{d^2 N / dp_T d\eta_{0-5\%}}{d^2 N / dp_T d\eta_{60-80\%}} \quad (2)$$

130 The vertical lines and horizontal lines in Fig. (4) represent the statistical errors and bin
 131 widths, respectively and the colored boxes the systematic uncertainties, while the error band
 132 at unity on the right side of the plot corresponds to the p_T independent uncertainty on N_{bin}
 133 scaling.

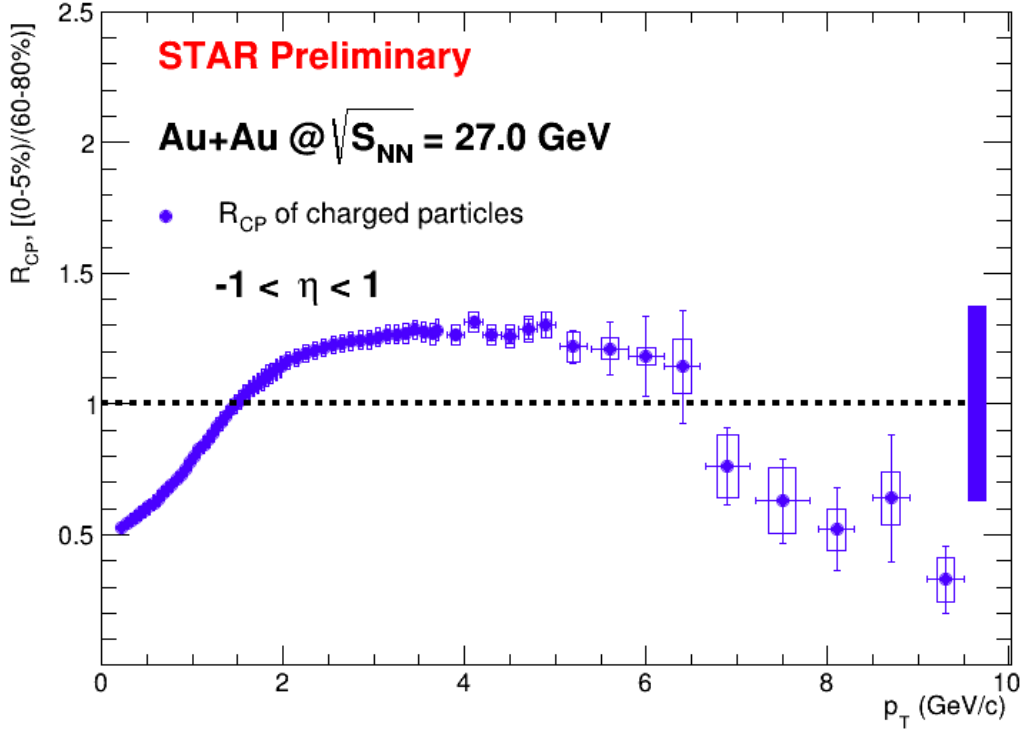


Figure 4: R_{CP} for inclusive charged particles at $\sqrt{s_{NN}} = 27$ GeV collision energy. The error band at unity on the right side of the plot corresponds to the p_T independent uncertainty on N_{bin} scaling. The vertical error bars correspond to statistical uncertainties and the colored boxes to the point-to-point systematic uncertainties.

134 The growth of R_{CP} is seen at low values of p_T (up to $p_T \approx 2$ GeV/c), which is affected by
 135 effects such as Cronin enhancement [19, 21, 25], radial flow [24], and the relative dominance
 136 of coalescence over fragmentation during hadronization [24]. However, as p_T increases, R_{CP}
 137 reaches a plateau and then demonstrates suppression of hadrons produced in central collisions
 138 with respect to peripheral collisions.

139 Conclusion

140 In this report, the nuclear modification factor R_{CP} for $Au+Au$ collisions at a collision energy
 141 of $\sqrt{s_{NN}} = 27$ GeV at the STAR experiment was presented. A significant extension to higher p_T
 142 values has been achieved. This advancement has enabled a more accurate characterization of the
 143 behavior of the nuclear modification in medium. Notably, suppression of particle production at
 144 high p_T is observed. However, the data is not sufficient to claim the formation of QGP based on
 145 this observable, and further study and investigation of the behavior of the nuclear modification
 146 factor dependence on energy on the data from STAR BES-II program are necessary. Future
 147 comparisons with hydrodynamic models may help interpret the presented data.

Acknowledgments

148

149 This work was supported by Russian Science Foundation under grant N 22-72-10028.

References

150

- 151 [1] L. Adamczyk et al. “Beam Energy Dependence of Jet-Quenching Effects in Au+Au
152 Collisions at $\sqrt{s_{\text{NN}}} = 7.7, 11.5, 14.5, 19.6, 27, 39,$ and 62.4 GeV”. In: *Phys. Rev. Lett.*
153 121.3 (2018), p. 032301. DOI: 10.1103/PhysRevLett.121.032301. arXiv: 1707.01988
154 [nucl-ex].
- 155 [2] I. Arsene et al. “Quark gluon plasma and color glass condensate at RHIC? The Perspective
156 from the BRAHMS experiment”. In: *Nucl. Phys. A* 757 (2005), pp. 1–27. DOI: 10.1016/
157 j.nuclphysa.2005.02.130. arXiv: nucl-ex/0410020.
- 158 [3] B. B. Back et al. “The PHOBOS perspective on discoveries at RHIC”. In: *Nucl. Phys.*
159 *A* 757 (2005), pp. 28–101. DOI: 10.1016/j.nuclphysa.2005.03.084. arXiv: nucl-
160 ex/0410022.
- 161 [4] John Adams et al. “Experimental and theoretical challenges in the search for the quark
162 gluon plasma: The STAR Collaboration’s critical assessment of the evidence from RHIC
163 collisions”. In: *Nucl. Phys. A* 757 (2005), pp. 102–183. DOI: 10.1016/j.nuclphysa.2005.
164 03.085. arXiv: nucl-ex/0501009.
- 165 [5] K. Adcox et al. “Formation of dense partonic matter in relativistic nucleus-nucleus colli-
166 sions at RHIC: Experimental evaluation by the PHENIX collaboration”. In: *Nucl. Phys.*
167 *A* 757 (2005), pp. 184–283. DOI: 10.1016/j.nuclphysa.2005.03.086. arXiv: nucl-
168 ex/0410003.
- 169 [6] Miklos Gyulassy and Larry McLerran. “New forms of QCD matter discovered at RHIC”.
170 In: *Nucl. Phys. A* 750 (2005). Ed. by D. Rischke and G. Levin, pp. 30–63. DOI: 10.1016/
171 j.nuclphysa.2004.10.034. arXiv: nucl-th/0405013.
- 172 [7] Brett McInnes. “Trajectory of the cosmic plasma through the quark matter phase dia-
173 gram”. In: *Phys. Rev. D* 93.4 (2016), p. 043544. DOI: 10.1103/PhysRevD.93.043544.
174 arXiv: 1506.05873 [hep-th].
- 175 [8] Edwin Laermann and Owe Philipsen. “The Status of lattice QCD at finite temperature”.
176 In: *Ann. Rev. Nucl. Part. Sci.* 53 (2003), pp. 163–198. DOI: 10.1146/annurev.nucl.53.
177 041002.110609. arXiv: hep-ph/0303042.

- 178 [9] Kenji Fukushima and Tetsuo Hatsuda. “The phase diagram of dense QCD”. In: *Rept. Prog.*
179 *Phys.* 74 (2011), p. 014001. DOI: 10.1088/0034-4885/74/1/014001. arXiv: 1005.4814
180 [hep-ph].
- 181 [10] J. Cleymans et al. “Comparison of chemical freeze-out criteria in heavy-ion collisions”.
182 In: *Phys. Rev. C* 73 (2006), p. 034905. DOI: 10.1103/PhysRevC.73.034905. arXiv:
183 hep-ph/0511094.
- 184 [11] Y. Aoki et al. “The Order of the quantum chromodynamics transition predicted by the
185 standard model of particle physics”. In: *Nature* 443 (2006), pp. 675–678. DOI: 10.1038/
186 nature05120. arXiv: hep-lat/0611014.
- 187 [12] A. Bazavov et al. “Chiral crossover in QCD at zero and non-zero chemical potentials”. In:
188 *Phys. Lett. B* 795 (2019), pp. 15–21. DOI: 10.1016/j.physletb.2019.05.013. arXiv:
189 1812.08235 [hep-lat].
- 190 [13] E. Scott Bowman and Joseph I. Kapusta. “Critical Points in the Linear Sigma Model with
191 Quarks”. In: *Phys. Rev. C* 79 (2009), p. 015202. DOI: 10.1103/PhysRevC.79.015202.
192 arXiv: 0810.0042 [nucl-th].
- 193 [14] Shinji Ejiri. “Canonical partition function and finite density phase transition in lattice
194 QCD”. In: *Phys. Rev. D* 78 (2008), p. 074507. DOI: 10.1103/PhysRevD.78.074507.
195 arXiv: 0804.3227 [hep-lat].
- 196 [15] Zachary Sweger. “Recent Results and Future Prospects from the STAR Beam Energy
197 Scan Program”. In: *57th Rencontres de Moriond on QCD and High Energy Interactions.*
198 May 2023. arXiv: 2305.07139 [nucl-ex].
- 199 [16] J. D. Bjorken. “Energy Loss of Energetic Partons in Quark - Gluon Plasma: Possible
200 Extinction of High $p(t)$ Jets in Hadron - Hadron Collisions”. In: (Aug. 1982).
- 201 [17] Miklos Gyulassy, Peter Levai, and Ivan Vitev. “Jet quenching in thin quark gluon plasmas.
202 1. Formalism”. In: *Nucl. Phys. B* 571 (2000), pp. 197–233. DOI: 10.1016/S0550-3213(99)
203 00713-0. arXiv: hep-ph/9907461.
- 204 [18] Michael L. Miller et al. “Glauber modeling in high energy nuclear collisions”. In: *Ann.*
205 *Rev. Nucl. Part. Sci.* 57 (2007), pp. 205–243. DOI: 10.1146/annurev.nucl.57.090506.
206 123020. arXiv: nucl-ex/0701025.
- 207 [19] J. W. Cronin et al. “Production of hadrons with large transverse momentum at 200, 300,
208 and 400 GeV”. In: *Phys. Rev. D* 11 (1975). Ed. by J. R. Smith, pp. 3105–3123. DOI:
209 10.1103/PhysRevD.11.3105.

- 210 [20] D. Antreasyan et al. “Production of hadrons at large transverse momentum in 200-, 300-,
211 and 400-GeV $p - p$ and p -nucleus collisions”. In: *Phys. Rev. D* 19 (3 Feb. 1979), pp. 764–
212 778. DOI: 10.1103/PhysRevD.19.764. URL: [https://link.aps.org/doi/10.1103/
213 PhysRevD.19.764](https://link.aps.org/doi/10.1103/PhysRevD.19.764).
- 214 [21] P. B. Straub et al. “Nuclear dependence of high- x_t hadron and high- τ hadron-pair pro-
215 duction in p-A interactions at $\sqrt{s} = 38.8$ GeV”. In: *Phys. Rev. Lett.* 68 (4 Jan. 1992),
216 pp. 452–455. DOI: 10.1103/PhysRevLett.68.452. URL: [https://link.aps.org/doi/
217 10.1103/PhysRevLett.68.452](https://link.aps.org/doi/10.1103/PhysRevLett.68.452).
- 218 [22] Ivan Vitev. “Initial state parton broadening and energy loss probed in d + Au at RHIC”.
219 In: *Phys. Lett. B* 562 (2003), pp. 36–44. DOI: 10.1016/S0370-2693(03)00535-5. arXiv:
220 nucl-th/0302002.
- 221 [23] Alberto Accardi and Miklos Gyulassy. “Cronin effect and geometrical shadowing in d+Au
222 collisions: pQCD versus colour glass condensate”. In: *Journal of Physics G: Nuclear and
223 Particle Physics* 30.8 (July 2004), S969. DOI: 10.1088/0954-3899/30/8/040. URL:
224 <https://dx.doi.org/10.1088/0954-3899/30/8/040>.
- 225 [24] V. Greco, C. M. Ko, and P. Levai. “Parton coalescence at RHIC”. In: *Phys. Rev. C* 68
226 (2003), p. 034904. DOI: 10.1103/PhysRevC.68.034904. arXiv: nucl-th/0305024.
- 227 [25] D. Antreasyan et al. “Production of Hadrons at Large Transverse Momentum in 200-GeV,
228 300-GeV and 400-GeV $p p$ and $p n$ Collisions”. In: *Phys. Rev. D* 19 (1979), pp. 764–778.
229 DOI: 10.1103/PhysRevD.19.764.